JOURNAL OF MATERIALS SCIENCE 33 (1998) 5573–5580

Effect of microgravity on grain coarsening during liquid phase sintering in the Fe–Cu system

J. NASER, J. E. SMITH JR
Consortium for Materials Development in Space and Department of Chemical & Materials Engineering, University of Alabama in Huntsville, Huntsville, AL, 35899, USA
E-mail: jesmith@ebs.330.eb.uah.edu

A. K. KURUVILLA
IITRI/MRF Building 4618, Marshall Space Flight Center, MSFC, AL 35812, USA

Samples within the Fe–Cu system with three different volume fractions of solid (50, 60 and 70 vol % Fe) and four different sintering times (2.5, 5, 17 and 66 min) were liquid phase sintered (LPS) in microgravity. Particle coarsening during LPS is generally known to increase with increasing volume fraction of solid. Contrary to expectations, there was an enhancement in particle coarsening with a decrease in the volume fraction of solid. The agglomerated microstructures observed in these samples (especially those with a lower volume fraction of solid) also exhibited a higher grain growth constant consistent with their higher 3D coordination number. The relevant analysis discussed in this paper strongly suggests that agglomeration is promoted by Brownian motion that dominates any density-driven force in the absence of gravity. The observed particle growth characteristics were in excellent agreement with the Lifshitz–Slyozov encounter modified theory, which incorporates the effect of higher solid volume fraction and particle coalescence into the LSW theory. The particle distributions appear to remain unchanged with processing time beyond 2.5 min, suggesting thereby, that agglomeration promotes an equilibrium particle configuration early on in the process and enables scaled grain growth with time.

1. Introduction

The coexistence of a liquid phase with solid particles is characteristic of LPS. During the process, larger particles grow at the expense of smaller particles in order to minimize the total interfacial surface energy of the system. This phenomenon is well known as Ostwald ripening [1]. Previous efforts in modelling the growth of solid particles dispersed in a liquid phase have centred around the well known Lifshitz–Slyozov and Wagner (LSW) [2, 3] theory. Since the LSW theory assumes a very small volume fraction of solid phase dispersed in the liquid matrix, the Lifshitz–Slyozov Encounter Modified (LSEM) model [4] has been developed to account for the effect of higher solid volume fractions and encounter between solid particles.

Typical LPS compositions for processing in unit gravity are dictated and/or limited by the density differences of the components. Solid volume fractions are high in order to prevent settling or floating of the particles and slumping of the LPS compact or part. As a result, the Ostwald ripening phenomenon cannot be readily studied on Earth without the interference of density driven settling forces. A microgravity environment, on the other hand, is attractive for understanding certain aspects of LPS, such as Ostwald ripening and particle coarsening in the absence of settling forces.

Solid particles in the liquid matrix during LPS are affected by several forces that cause their motion, examples of which are: (i) the gravitational force; (ii) Brownian motion, which is defined as the random thermal motion of suspended particles that are sufficiently large to be observed [5]; and (iii) convection forces due to temperature gradients. In the case of LPS experiments performed on Earth, the gravitational force is the dominant force that causes particle motion. In contrast, Brownian motion might be the dominant force in the absence of gravity.

The contact time (the time required for two separated particles in the liquid matrix to contact each other) for particle contact will depend on the force that drives the particles in the liquid matrix. Haller [6] estimated the number of contacts expected for random monosized spheres in a matrix phase of a two-phase system to be

$$N_c = -8\ln(1 - V_s) \quad (1)$$

where V_s is the solid volume fraction and N_c is the estimated number of contacts between the particles. Assuming that the particles are arranged in an idealized cubic array, the spacing between two particles can be estimated from the following equation [7]

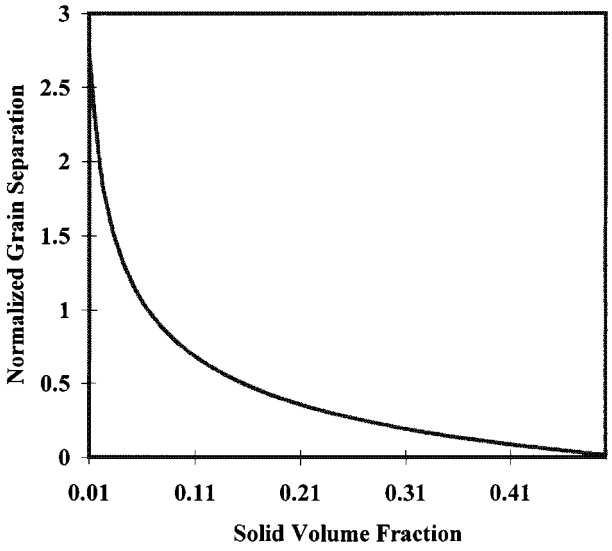

Figure 1 Normalized grain separation versus solid volume fraction [7].

$$\lambda = D\left[\left(\frac{\pi}{6V_s}\right)^{1/3} - 1\right] \tag{2}$$

where λ is the separation between grain surfaces, V_s is the solid volume fraction and D is the grain diameter. The relationship between the normalized grain separation, λ/D, and the solid volume fraction is presented in Fig. 1. Clearly, an increase in the solid volume fraction contributes to a decrease in the grain separation. Hence, an increase in the volume fraction of solid could be expected to enhance grain coarsening.

1.1. Gravitational force

In the presence of a gravitational force, the settling velocity for solid particles in a liquid matrix can be calculated from Stokes' law, according to the following equation

$$v = \frac{aD^2(\rho_s - \rho_l)}{18\eta} \tag{3}$$

where a is the gravitational acceleration, D is the particle diameter, ρ_s and ρ_l are solid and liquid densities, respectively, and η is the liquid viscosity. Therefore, the time required for a particle to travel the separation distance, λ, can be derived from Equations 2 and 3 as

$$\tau_s = \frac{18\eta\lambda}{aD^2(\rho_s - \rho_l)} \tag{4}$$

where τ_s is the average time for settling of a grain of density ρ_s and diameter D.

1.2. Brownian motion

In considering Brownian motion, according to Einstein's treatment [8], the mean displacement, χ, of a grain can be calculated as

$$\chi^2 = \frac{2kTt}{3\pi\eta D} \tag{5}$$

where k is the Boltzmann constant, T is the absolute temperature, t is the time, η is the liquid viscosity and D is the grain diameter. Rearranging for t in the above equation

$$\tau_B = \frac{3\pi D\eta\lambda^2}{2kT} \tag{6}$$

where τ_B is settling time as a result of Brownian motion and all the other terms are as previously described.

This paper discuses the results of LPS experiments in microgravity as they are analysed in the light of the differences in the contact time as a function of the active forces with and without gravity.

2. Experimental procedure

Three compositions, Fe–33 wt % Cu, Fe–43 wt % Cu and the Fe–53 wt % Cu were liquid phase sintered on sounding rocket and space shuttle missions. These compositions enabled evaluation of LPS with 50, 60 and 70 vol % solid, respectively. Both the Fe and Cu powders were obtained from Alfa *AESAR*. The Fe powder was 99.9% pure, with a mean particle diameter of 6–9 μm and the Cu powder was 99% pure with a mean particle diameter of 8–11 μm. These powders were mixed, without any lubricant additions, in an axial rotary mixer where the rotational speed was optimized using the equation r.p.m.$= 32/(\text{cylinder diameter})^{1/2}$ [9]. The blended powders were pressed to form a green compact in a die lubricated with zinc sterate, following which they were reduced in a tubular reactor under a flow of high purity hydrogen. The average size of these compacts was 10 mm height and 18.8 mm diameter. The time–temperature profile for reduction was designed to minimize solid state sintering while reducing oxides and lubricants from the compacts. This involved gradual heating up to 300 °C with hold times of 30 min at 50, 115, 150, 200, 250 and 300 °C. Finally, the reduced samples were stacked in a cylindrical stainless steel ampoule, separated by stainless steel shims. The ampoules were loaded into the ECLiPSE sintering furnace, which was integrated into the flight hardware for LPS in microgravity. LPS experiments were conducted in an argon environment (82.7 KPa pressure) using an automated isothermal furnace. The heating rate was 7 K min^{-1}. LPS was performed at 1110 °C for varying periods of time on the different missions. These processing times of 2.5, 5, 17 and 66 min represented times during which Cu remained in the molten state. Further details pertaining to flight hardware and processing have been published elsewhere [10–13]. Sintered samples were first sectioned using an abrasive cutoff wheel. One section was hot press mounted using bakelite. The mounted samples were ground using 120, 240, 320 and 400 grit SiC abrasive paper. Fine polishing was accomplished on a polishing wheel using 240, 400 and 600 grit alumina paste in H_2O. Finally, they were all ultrasonically cleaned in distilled water before metallographic examination. [13].

TABLE I Effect of sintering time and solid volume fraction on particle size

Sintering time (min)	Solid volume fraction, $R(\mu)$		
	50 vol % Fe	60 vol % Fe	70 vol % Fe
2.5	7.99	8.13	5.28
5	8.03	8.27	7.52
17	9.37	8.58	8.10
66	13.17	12.41	10.65

3. Results and discussion

3.1. Particle coarsening

In the microstructural analysis of the samples, at least ten different sites were randomly selected and their images captured digitally using Sigma Scan software. The radii of more than 600 particles were determined for each of the samples by measuring the area and assuming that the particles were spherical. Table I shows the mean grain size (radii) for the different specimens examined.

In general, the coarsening models predict that the cube of the particle size is a linear function of the sintering time [2–4, 14–18]. Accordingly, the cube of the mean particle size (radius) for each volume fraction was plotted against the sintering time. The results are presented in Fig. 2 for the solid volume fractions 50, 60 and 70% Fe, respectively. The data were fitted to a first order function that represented the best fit.

The grain growth constant steadily increased with decreasing volume fraction of solid. A decrease in the grain separation distance with increasing volume fraction of solid should have resulted in an attendant increase in the growth constant. The unexpected variation in the growth constant, contrary to expectations based on past studies suggests that there are other factors operational in microgravity. The most likely possibility is that of agglomeration. If particles agglomerated in the absence of gravitational force, it would be expected that the growth constant would increase with agglomeration.

Based on the observed relationship between the growth constant and the volume fraction of solid, it appears that the agglomeration tendency increases with decreasing solid volume fraction. This appears to be reasonable because the higher volume fraction of solid would generate a skeletal structure that inhibits particle movement and agglomeration. As shown in Fig. 1, the normalized grain separation distance becomes extremely small, providing an interconnected network of grains when the volume fraction of solid exceeds 50%. Accordingly, agglomeration will be enhanced when there is a decrease in the number of particle contacts and rigidity of the skeletal structure that accompanies decreasing solid volume fractions. The following is a discussion of this phenomenon.

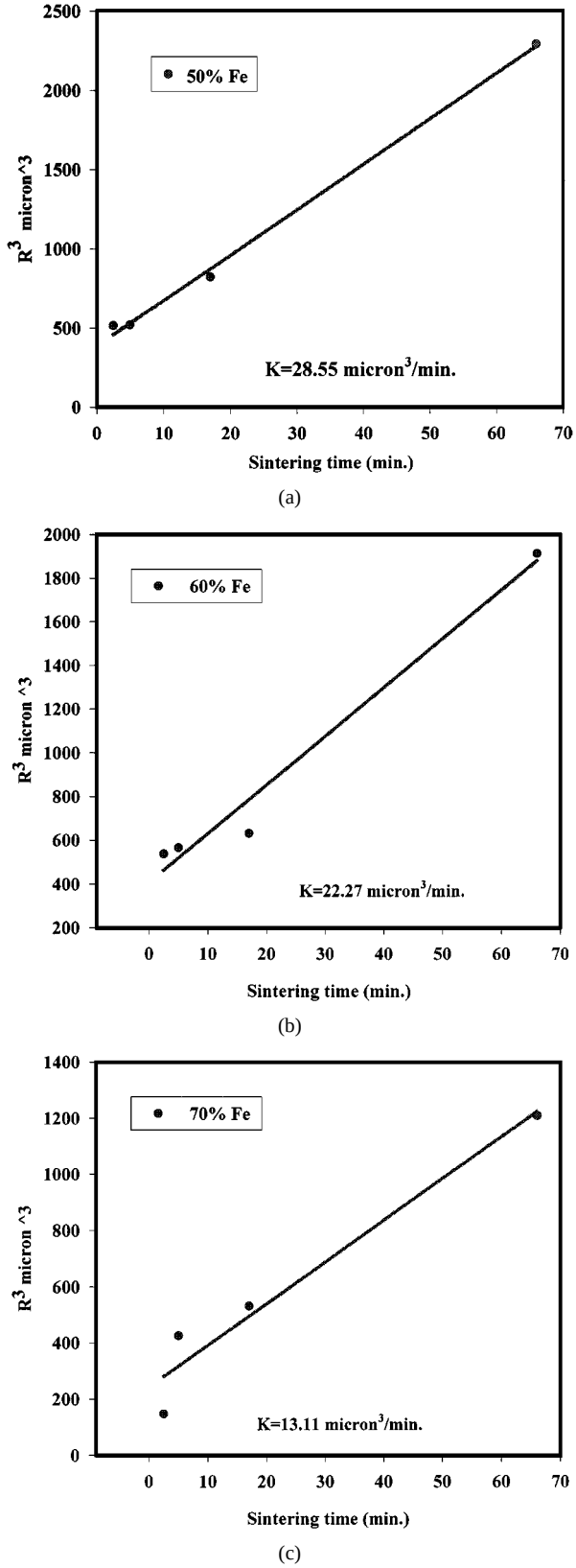

Figure 2 The effect of sintering time on grain growth for solid volume fractions of (a) 50, (b) 60, and (c) 70% Fe.

3.2. Particle agglomeration

Agglomeration in solid–liquid mixtures has been observed in Earth-based LPS samples [19–26]. This was attributed to settling as a result of gravitational force as well as weak interaction forces. The settling of solid particles in unit gravity complicates the experimental testing of coarsening theories, since all these theories assume stationary solid particles in the liquid matrix [7]. Several researchers [27–37] have suggested that microgravity will be the right environment to examine coarsening theories in the absence of settling and convection forces that cause grain contact. However, such

experiments will have to guarantee that there is a dispersion of spherical grains with minimal contact and coalescence during the coarsening process. The numerous observations of grain agglomeration and coalescence [28, 38–44] observed in microgravity experiments along with that in the present study suggest that experiments in microgravity may not be the best setting to examine coarsening theories. In the present work, grain agglomeration was clearly observed in the microgravity processed 50% Fe samples. Liquid pools of copper along with agglomerated areas of solid particles can be observed in Fig. 3a, b.

It would be expected that high volume fractions of solid would preclude any movement of solid and thus limit agglomeration. Accordingly, agglomeration would be most pronounced in the 50% solid volume fraction sample among the three compositions studied here. As is readily seen in Fig. 1, the grain separation distance is extremely small in samples with high volume fraction (greater than 50%) of solid. Therefore, agglomeration would be expected to be pronounced only in samples with solid volume fractions of less than or equal to 50%. Interestingly, coalescence was also frequently observed in the microstructure of this sample with a solid volume fraction of 50% as shown in Fig. 4.

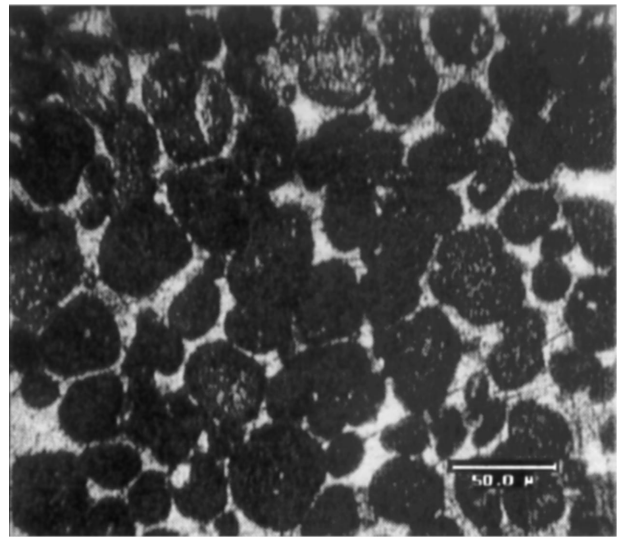

Figure 4 Coalesced particles from the 50 vol % Fe specimen.

This is clear indication of grain motion in the absence of a gravitational force. Agglomeration results in an increase in the localized solid volume fraction and 3D coordination number. This, in turn, promotes coalescence in the agglomerated zones for those specimens. In the absence of gravitational force, Brownian motion is believed to be responsible for grain agglomeration. The following discussion further strengthens this argument.

Figs 5 and 6 show the effect of gravitational force on the contact time and the relative influence of Stokes' settling and Brownian motion. The contact times were not calculated past a solid volume fraction of 0.5 because it has been found that solid particle contact precludes the free movement of particles either due to Stokes' settling or Brownian motion at these high volume fractions of

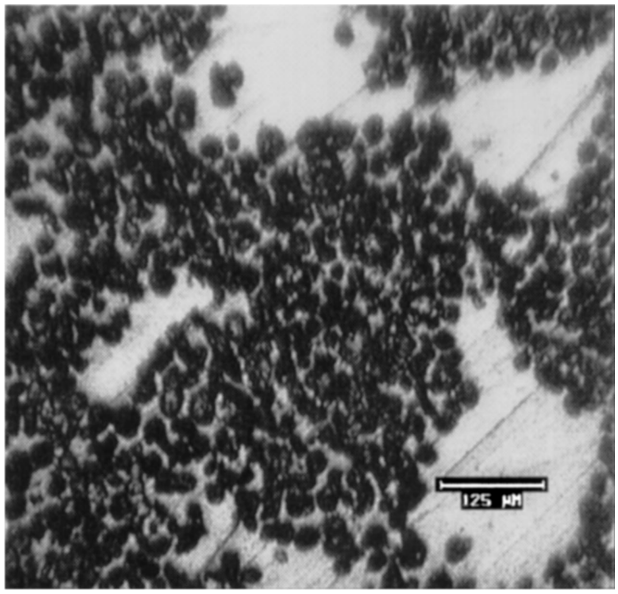

(a)

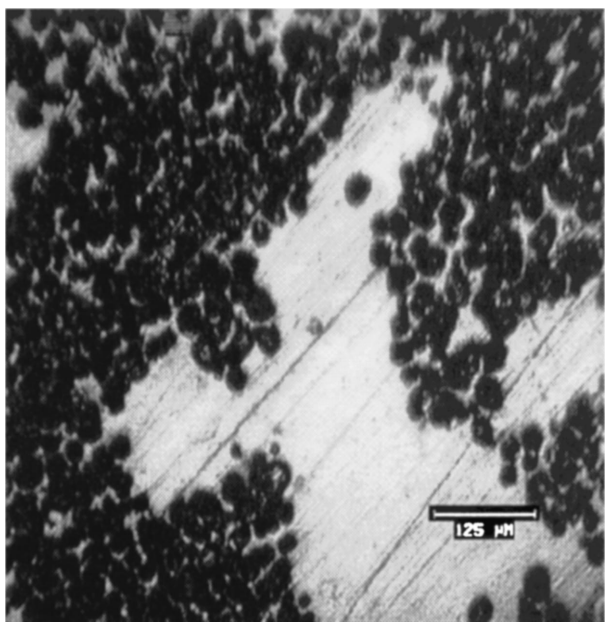

(b)

Figure 3 Some of the agglomerated areas (a) and liquid copper pools (b) observed in the 50% Fe specimen.

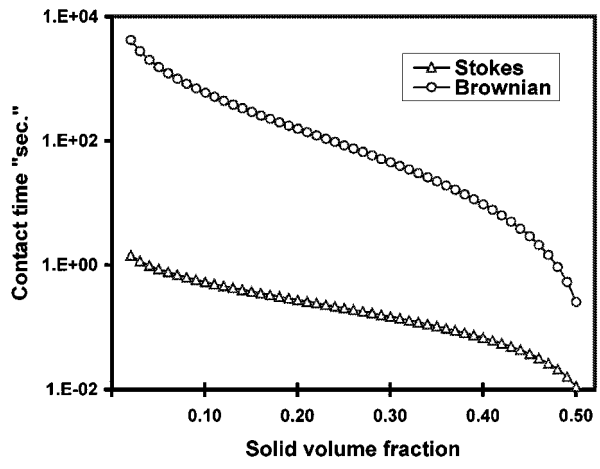

Figure 5 Contact time between Fe particles for Stokes' versus Brownian motion under unit gravity.

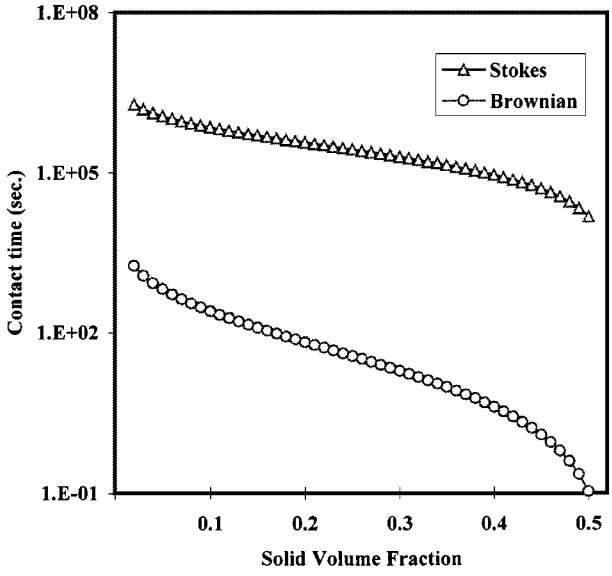

Figure 6 Contact time between Fe particles for Stokes' versus Brownian motion in microgravity.

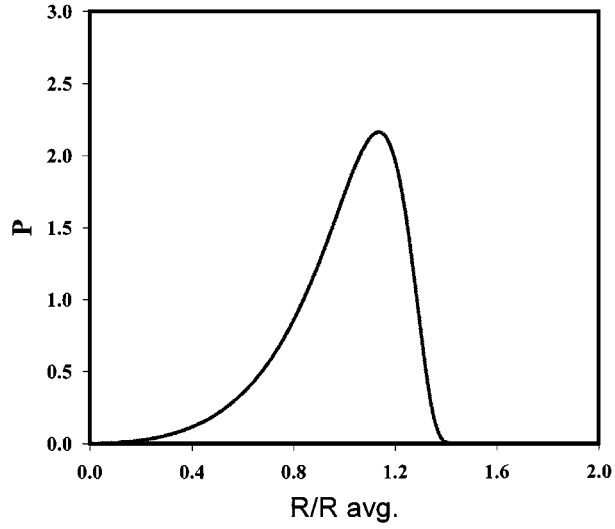

Figure 7 LSW normalized particle size distribution.

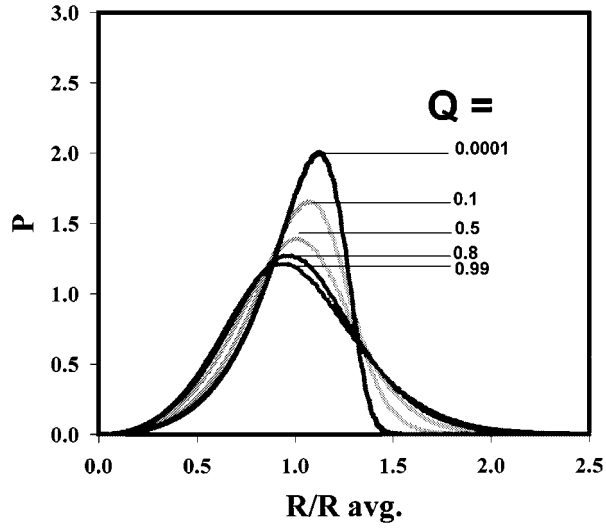

Figure 8 LSEM predicted grain size distributions corresponding to different solid volume fractions [4].

solid [7]. As is clear from Fig. 5, Stokes' settling is the dominant force that contributes to the shorter contact time in unit gravity. In contrast, as seen in Fig. 6, Brownian motion is the dominant force that promotes the shorter contact time in microgravity. These graphs were constructed using Equations 4 and 6, which were presented earlier in this paper. These results are consistent with other observations in which grain agglomeration and coalescence have been observed in microgravity experiments involving solid grains in liquids, liquid droplets in liquid and solid grains in vapour [28, 38–44].

3.3. Modelling particle growth

Lifshitz and Slyozov [2] and Wagner [3] predicted the grain growth behaviour of two phase systems in which a solid phase is dispersed in a liquid matrix. Their classical work is well known as the LSW theory. In their work, they were able to solve analytically for (i) the growth of the mean particle size with time, and (ii) the asymptotic normalized particle size distribution of the solid phase (Fig. 7). However, their work involved some major assumptions to simplify the problem. One of the main assumptions was that the solid volume fraction is very small (tending towards zero). Since LPS systems have large volume fractions of solid, the LSW model is not directly applicable to this process.

Davies *et al*. [4] modified the LSW theory to include the effect of solid volume fraction and the encounter of particles. In this modified version, which is called the LSEM theory, the LSW continuity equation was modified by adding an encounter term on the right-hand side of the equation. This term represents the number of particles entering and leaving a certain grain size class as a result of encounter between two particles. Their predicted distributions were wider than those predicted based on the LSW theory and the distribution width was proportional to the solid volume fraction (Fig. 8).

In comparing the experimental and predicted grain size distributions in this study, the predicted grain size distribution based on the LSW model did not correlate well with the experimental grain size distributions of the Fe–Cu system as shown in Fig. 9 for the 50% solid volume fraction. The main reason for this poor agreement can be attributed to the assumption of an extremely small solid volume fraction in the LSW model.

A comparison of the experimental grain size distributions and the predicted grain size distributions based on the LSEM theory for corresponding volume fractions of solid is presented in Fig. 10.

The experimental and predicted distributions were tested by the chi-squared test [45], which indicates the closeness of the distributions. According to the chi-squared test

$$\aleph^2 = \frac{\sum_{i=1}^{k} [(z_1)_i - (z_2)_i]^2 / (z_2)_i^2}{k-1} \qquad (7)$$

where k is the number of intervals the results were grouped into, z_{1_i} is the measured number in the interval

TABLE II Experimental observations agree well with the LSEM model

Solid volume fraction (% Fe)	$\aleph^2$	Agreement (%)
50	0.66	99
60	2.79	95
70	0.67	99

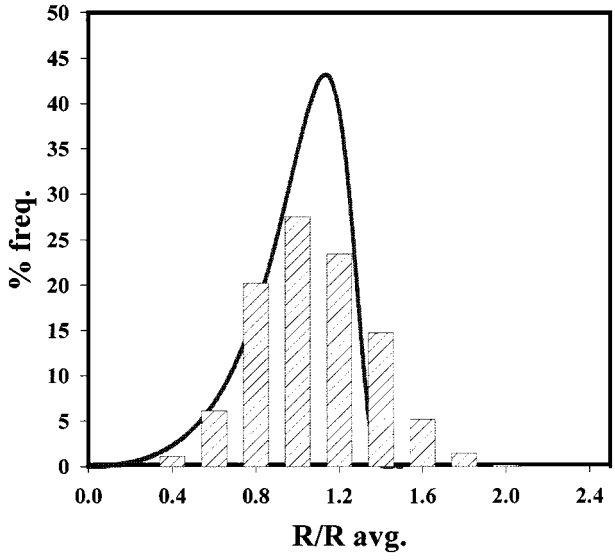

Figure 9 LSW model versus 50% Fe solid volume fraction.

of the experimental set, and z_{2_i} is the theoretical value predicted by the model. Comparison of the calculated values of $\aleph^2$ (Table II) to the chi-squared table, indicates that agreement between the experimental results and the model is better than 95%.

This is further supported by the observation of a large number of coalesced particles in the Fe–Cu microstructure (Fig. 4), which had been considered in the LSEM coarsening model.

The grain size distribution appears to indicate that the volume fraction does not have a pronounced effect at least in the ranges considered in this study. Given that the degree of agglomeration increases with decreasing solid volume fraction, it could be speculated that the localized (agglomerated) grain size distribution might not change with solid volume fraction in microgravity as it does in experiments on Earth.

3.4. Particle size distribution

The normalized grain size distribution for more than 600 grains in each of the specimens was constructed for each sintering time. Fig. 11 represents the distributions for the four sintering times for the 50% Fe sample compared with the predicted LSEM distribution for the 0.5 solid volume fraction.

It appears that there is no significant difference between the normalized grain size distributions of the four sintering times. In addition, the shape of the normalized grain size distribution appears to have developed as early as 2.5 min into the sintering process. This can be attributed to agglomeration, which promotes an

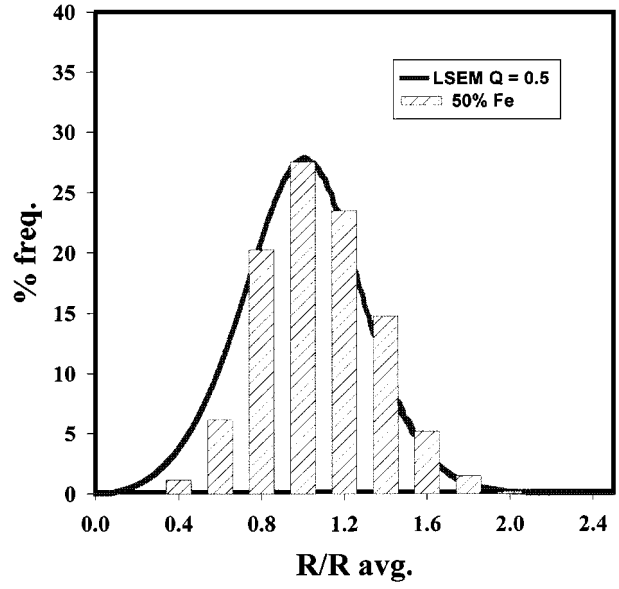

(a)

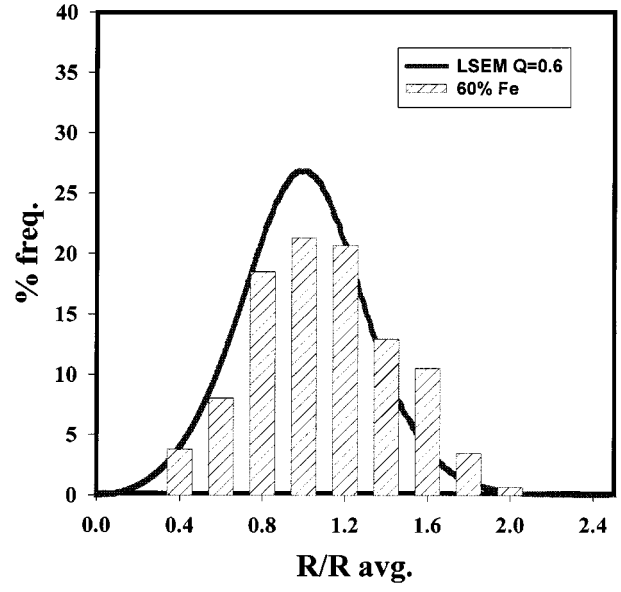

(b)

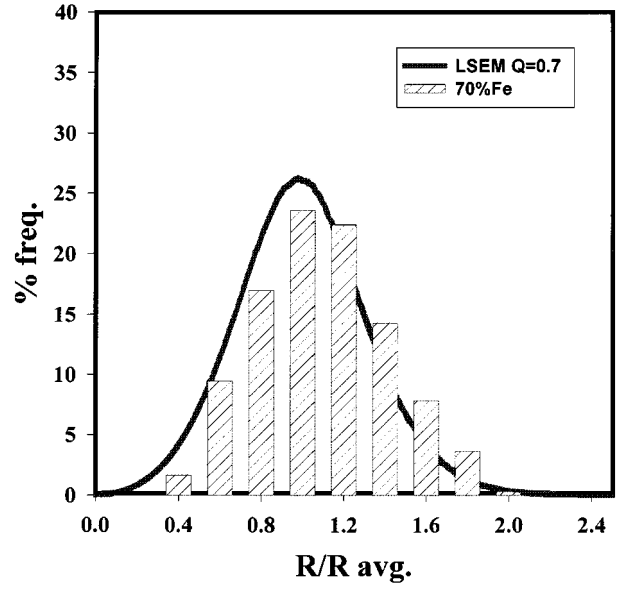

(c)

Figure 10 Comparison of predicted LSEM and observed grain size distributions in samples of solid volume fractions of (a) 50, (b) 60, and (c) 70% Fe.

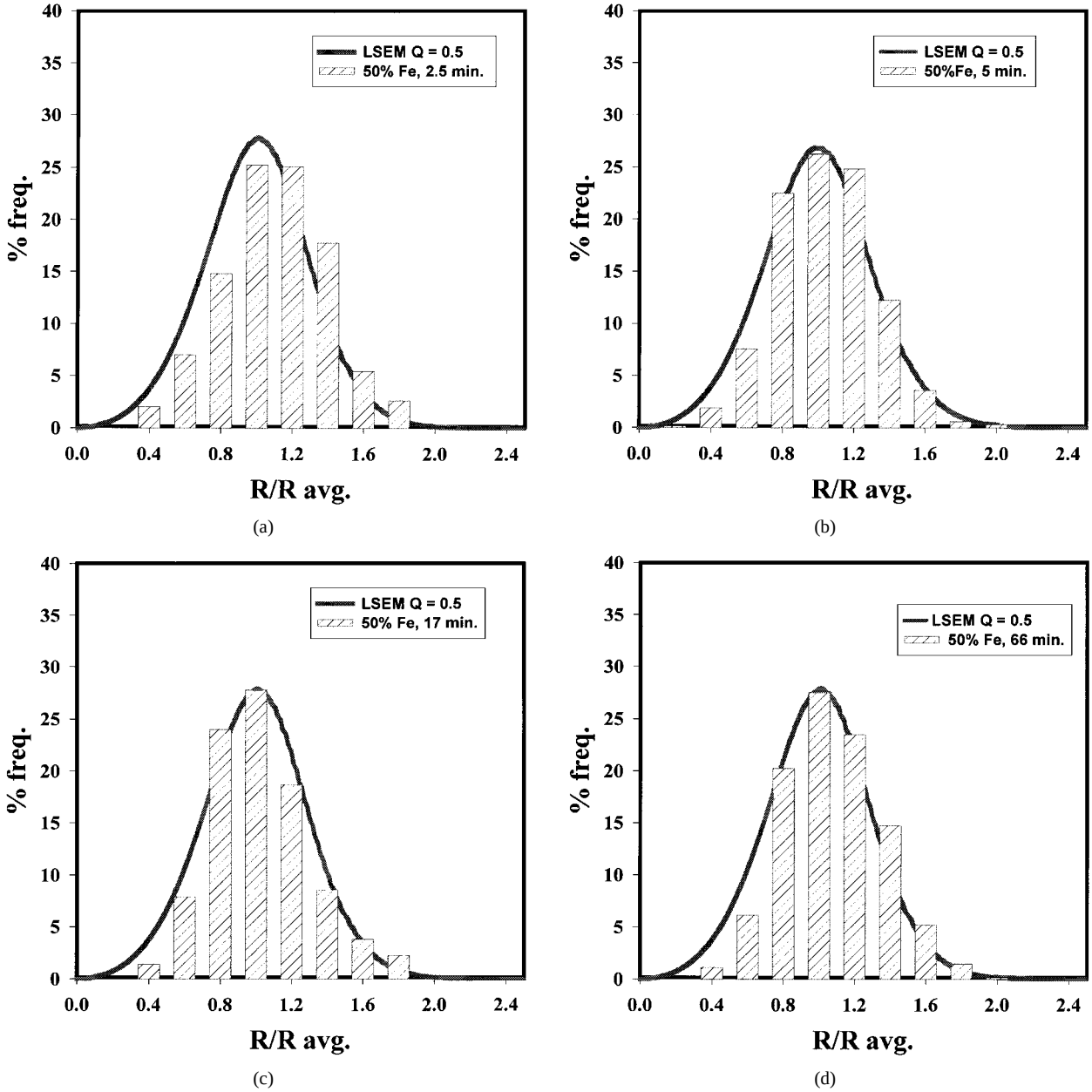

Figure 11 Grain size distribution of LSEM for solid volume fraction of 0.5 compared with the 50 vol % Fe experimental distributions for the sintering times of (a) 150 s, (b) 5 min, (c) 17 min, and (d) 66 min.

equilibrium particle configuration early on in the process. The similarity of the grain size distributions for sintering times ranging from 2.5 min to 66 min suggests that a scaled grain growth process was operative in these samples. This is similar to the observations during LPS in a Pb–Sn system [46], in which different scaled particle images at three different sintering times displayed similar grain size distribution.

4. Conclusions

The effect of microgravity on grain coarsening in the Fe–Cu system has been examined. In the absence of gravitational force, Brownian motion was believed to promote agglomeration of the solid phase. The contact times resulting from Brownian motion and Stokes' settling strongly suggest that Brownian motion is the dominant force that drives agglomeration. The grain growth constant steadily increases with decreasing solid volume fraction, consistent with the agglomeration, which begins to be pronounced in LPS samples with solid volume fractions equal to or less than 50%. Above a solid volume fraction of 50%, there is sufficient contact between the solid particles, which precludes the movement of particles for agglomeration. The microstructure, with a dispersion of agglomerated grains in pools of liquid copper, also substantiates the foregoing arguments. Excellent agreement was observed between the experimental distribution in this study and those predicted based on the LSEM model. This agreement is attributed to the inclusion of the effect of solid volume fraction on the grain size distributions and particle coalescence during the LPS process.

Acknowledgements

This work was supported by NASA under grant NAGW-812 to the Consortium for Materials Development in Space at The University of Alabama in Huntsville. Engineering support was also provided by

Wyle Laboratories and Teledyne Advanced Materials. The assistance provided by C. K. L. Davies, P. Nash and R. N. Stevens with the LSEM model is gratefully acknowledged. Numerous individuals from both academia and corporate industrial partners lent their knowledge, cooperation and support throughout this project.

References

1. W. OSTWALD, *Z. Phys. Chem.* **34** (1900) 495.
2. I. M. LIFSHITZ and V. V. SLYOZOV, *J. Phys. Chem. Solids* **19** (1961) 35.
3. C. WAGNER, *Z. Elektrochem.* **65** (1961) 581.
4. C. K. L. DAVIES, P. NASH and R. N. STEVENS, *Acta Metall.* **28** (1980) 179.
5. R. F. PROBSTEIN, in "Physicochemical Hydrodynamics: An Introduction," 2nd ed. (J. Wiley, London, 1994) p. 116.
6. W. HALLER, *J. Chem. Phys.* **42** (1965) 686.
7. R. M. GERMAN and Y. LIU, *J. Mater. Synthesis Process.* **4J** (1996) 23.
8. A. EINSTEIN, in "Investigations on the Theory of the Brownian Movement" (Dover, New York, 1956).
9. R. M. GERMAN, in "Powder Metallurgy Science" (Metallurgy Powder Industries Federation, NJ, 1984).
10. S. L. NOOJIN, J. G. VANDEGRIFT, K. L. HARTMAN and J. E. SMITH JR, *ASME Heat Transfer Div. Publ. HTD* **259** (1993) 127.
11. J. G. VANDEGRIFT, S. L. NOOJIN, K. L. RYAN, Z. XUE and J. E. SMITH JR, in Proceedings of the Seventh International Symposium on Experimental Methods for Microgravity Materials Science, edited by TMS, Warrendale, PA, 1995, p. 79–86.
12. Z. XUE, J. G. VANDEGRIFT and J. E. SMITH JR, *Microgravity Sci. Tech. Int. J. Microgravity Res. Appl.* **VIII/2**, (1995) 112.
13. Z. XUE, MSc. thesis, University of Alabama in Huntsville (1995) p. 35.
14. G. W. GREENWOOD, *Acta Metall.* **14** (1956) 243.
15. A. D. BRAILSFORD and P. WYNBLATT, *ibid.* **27** (1979) 489.
16. A. J. ARDELL, *ibid.* **20** (1972) 61.
17. K. TSUMURAYA and Y. MIYATA, *ibid.* **31** (1983) 437.
18. P. W. VOORHEES and M. E. GLICKSMAN, *ibid.* **32** (1984) 2013.
19. Y. LIU, D. F. HEANEY and R. M. GERMAN, *Acta Metall. Mater.* **43** (1995) 1687.
20. T. H. COURTNEY and J. K. LEE, *Metall. Trans.* **11A** (1980) 943.
21. A. N. NIEMI and T. H. COURTNEY, *Acta Metall.* **31** (1983) 1391.
22. A. P. PHILIPSE, B. C. BONEKAMP and H. J. VERINGS, *J. Amer. Ceram. Soc.* **73** (1990) 2720.
23. L. BERGSTROM, C. H. SCHILLING and I. A. AKSAY, *ibid.* **75** (1992) 3305.
24. S. G. SHABCSTARI and J. E. GRUZLESKI, *Metall. Mater. Trans.* **26A** (1995) 999.
25. R. M. GERMAN, *ibid.* **26A** (1995) 279.
26. P. W. VOORHEES and R. J. SCHAEFER, *Acta. Metall.* **35** (1987) 327.
27. P. W. VOORHEES, in "Coarsening in Solid–Liquid Mixtures" (North Western University, Evanston, IL, unpublished Science Requirements Document presented to NASA Lewis Research Center, June, 1994).
28. L. B. EKBOM, *Int. J. Refract. Hard Met.* **6** (1987) 231.
29. L. B. EKBOM and A. ELIASSON, in "Tungsten and Tungsten Alloys 1992," edited by A. Bose and R. J. Dowding (Metal Powder Industries Federation, NJ, 1993) p. 97.
30. A. ELIASSON, Ph.D. thesis, Royal Institute of Technology, Stockholm, Sweden (1992).
31. F. WEINBERG, *Metall. Trans.* **15B** (1984) 479.
32. C. M. KIPPHUT, T. KISHI, A. BOSE and R. M. GERMAN, in "Progress in Powder Metallurgy," Vol. 43 (Metal Powder Industries Federation, NJ, 1987) p. 93.
33. D. UFFELMAN, W. BENDER, L. RATKC and B. FEUERBACHER, *Acta Metall. Mater.* **43** (1995) 173.
34. T. MOOKHERJI, W. B. MCANCELLY and E. C. MCKANNAN, in Proceedings of the Third Space Processing Symposium: Skylab Results, Vol. 11, NASA Marshall Space Flight Center, AL, 1974, p. 963.
35. A. KENEISSL and H. FISCHMEISTER, in Material Sciences Under Microgravity, Results of Spacelab-1 ESA SP-222 (European Space Agency, France, 1984) p. 63.
36. L. RATKC, H. FISCHMEISTER and A. KNEISSL, in Proceedings of the Sixth European Symposium on Material Sciences Under Microgravity Conditions. ESA Sp-256 (European Space Agency, France, 1987) p. 161.
37. S. KOHARA and M. HOSHINO, in "Advances in Powder Metallurgy and Particulate Materials 1994," Vol. 3 (Metal Powder Industries Federation, NJ, 1994) p. 295.
38. F. BARBICRI, C. PATUELLI, P. GONNDI and R. MONTANARI, in Materials Sciences Under Microgravity, Results of Spacelab-1. ESA SP-222 (European Space Agency, France, 1984) p. 101.
39. J. K. BAIRD, in *ibid.* p. 319.
40. H. OTTO, in *ibid.* p. 379.
41. H. U. WALTER, in "Materials Science in space," edited by B. Feuerbacher, H. Hamacher and R. J. Neumann (Springer-Verlag, Germany, 1986) p. 343.
42. J. R. ROGERS and R. H. DAVIS, *Metall. Trans.* **21A** (1990) 59.
43. D. E. BROOKS, S. B. BAMBERGER, J. M. HARRIS, J. VAN ALSTINE and R. S. SNYDER, in Proceedings of the Sixth European Symposium on Material Sciences Under Microgravity Conditions. ESA SP-256 (European Space Agency, France, 1987) p. 131.
44. J. R. MARSHALL, in Joint Launch One Year Science Review of USML-1 and USMP-1, II, NASA Conference Publication 3272 (NASA Marshall Space Flight Center, AL, 1994).
45. E. E. HANS and P. H. HANS, in "Quantitative Image Analysis of Microstructures" (1988) p. 160.
46. S. C. HARDY and P. W. VOORHEES, *Metall. Trans.* **19A** (1988) 2713.

Received 1 June
and accepted 4 August 1998